Journal of Biomolecular NMR, **18:** 23–31, 2000.
KLUWER/ESCOM

Direct measurement of ^{1}H-^{1}H dipolar couplings in proteins: A complement to traditional NOE measurements

F. Tian, C.A. Fowler, E.R. Zartler, F.A. Jenney Jr., M.W. Adams & J.H. Prestegard*
Complex Carbohydrate Research Center, University of Georgia, Athens, GA 30602–4712, U.S.A.

Received 7 April 2000; Accepted 22 June 2000

Key words: CT-COSY, ^{1}H-^{1}H residual dipolar coupling, protein structure

Abstract

An intensity-based constant-time COSY (CT-COSY) method is described for measuring ^{1}H-^{1}H residual dipolar couplings of proteins in weakly aligned media. For small proteins, the overall sensitivity of this experiment is comparable to the NOESY experiment. In cases where the ^{1}H-^{1}H distances are defined by secondary structure, such as $^1H^{\alpha}$-$^1H^{N}$ and $^1H^{N}$-$^1H^{N}$ sequential distances in α-helices and β-sheets, these measurements provide useful orientational constraints for protein structure determination. This experiment can also be used to provide distance information similar to that obtained from NOE connectivities once the angular dependence is removed. Because the measurements are direct and non-coherent processes, such as spin diffusion, do not enter, the measurements can be more reliable. The $1/r^3$ distance dependence of directly observed dipolar couplings, as compared with the $1/r^6$ distance dependence of NOEs, also can provide longer range distance information at favorable angles. A simple 3D, ^{15}N resolved version of the pulse sequence extends the method to provide the improved resolution required for application to larger biomolecules.

Introduction

Recent progress in the sequencing of genes is placing increasing demands on the efficiency of structure determination methodology, whether by X-ray crystallography or NMR (Sali and Kuriyan, 1999). For NMR, some additional challenges exist in that some of the proteins coded by genes will not express or refold at levels suitable for the labeling required in most triple resonance experiments. These facts suggest reconsideration of the value of NMR experiments that require little (^{15}N only) or no isotopic labeling and incorporate new sources of structural information such as residual dipolar couplings. We consider here an experiment that measures ^{1}H homonuclear dipolar couplings and compare its performance to a traditional NOE experiment on two small proteins at natural abundance and labeled only with ^{15}N. Data from both a 2D homonuclear version and a 3D ^{15}N resolved version of the experiment are presented.

Measurement of inter-proton NOEs is widely recognized as the foundation of biomolecular structure determination by NMR (Wüthrich, 1986), yet there are several reasons that we should consider replacing or supplementing these experiments. For example, NOEs in large molecules suffer from spin diffusion, making their quantitative interpretation difficult. The steep distance dependence of NOEs makes relationships between remote parts of molecules hard to determine, and the basic dependence of NOEs on both correlation time and distance complicates interpretation in the presence of anisotropic or internal motions.

A possible source of information to supplement NOEs is the direct measurement of dipolar couplings in oriented media (Tolman et al., 1995; Tjandra and Bax, 1997; Clore et al., 1998; Prestegard, 1998). Several potential advantages are associated with the use of dipolar coupling data. Because dipolar coupling measurements are direct, non-coherent transfer processes, such as spin diffusion, do not complicate interpreta-

*To whom correspondence should be addressed. E-mail: jpresteg@ccrc.uga.edu

tion. Dipolar couplings depend on both distance and orientation, and the angular information can provide additional long range structural constraints. Finally, the effects of motion on directly measured dipolar couplings are less complex, making structural interpretation in the presence of motion possible. These advantages have been clearly illustrated using dipolar couplings between directly bonded pairs of nuclei. Some very efficient experiments for collecting these data now exist (Tolman and Prestegard, 1996; Tjandra and Bax, 1997; Ottiger et al., 1998; Wang et al., 1998).

Despite the potential advantages, there are a few drawbacks to heavy reliance on residual dipolar couplings. Among them is the fact that there is not a one-to-one mapping of measured dipolar couplings to orientational angles, and several independent measurements of couplings within a single rigid fragment must be made to allow the definition of structure. At first glance it may seem possible to acquire sufficient data using only ^{15}N-^{1}H one-bond couplings by defining a rigid fragment as a secondary structure element having many N-H bonds. However, for both α-helices and β-sheets, N-H bonds are nearly parallel to one another, and measurements with very high precision are required for sufficiently independent determination of a unique orientation.

One possibility is to supplement ^{15}N-^{1}H dipolar data with intra- and interresidue $^{1}H^{N}$-$^{1}H^{\alpha}$ and $^{1}H^{N}$-$^{1}H^{N}$ couplings. The vectors connecting these protons in α-helices and β-sheets are not parallel to the backbone ^{15}N-^{1}H amide vectors, and interactions involving these pairs of nuclei nicely complement ^{15}N-^{1}H one-bond coupling data. The ability to detect these couplings has already been demonstrated (Tjandra and Bax, 1997; Cai et al., 1999; Pellecchia et al., 2000; Peti and Griesinger, 2000). Here we extend these observations and attempt a more quantitative analysis.

We recently presented a simple method for the direct measurement of through-space dipole–dipole couplings among protons in an oligosaccharide (Tian et al., 1999). This method was based on the use of 2D constant time coupling correlated spectroscopy (CT-COSY) in media that partially align dissolved molecules in the presence of a magnetic field. Here we illustrate the applicability of these methods to problems in protein structure determination and extend the methods to a 3D, ^{15}N edited version that offers the improved resolution required for this application. We show that homonuclear ^{1}H dipolar interactions can be measured with a sensitivity that is, on average, comparable to measurements of NOE interactions.

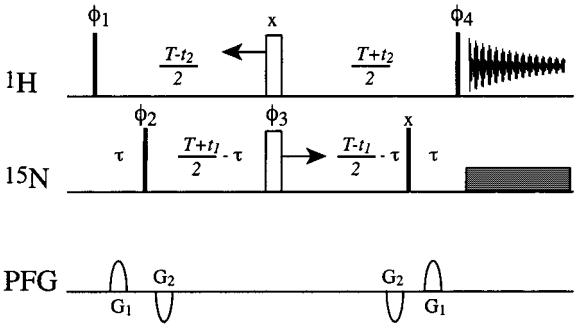

Figure 1. Pulse sequence for the 3D ^{15}N-resolved CT-COSY experiment. Pulses of 90° and 180° are represented by filled and open bars, respectively. Phase cycling was as follows: Φ_1 = x, −x; Φ_2 = 2x, 2(−x); Φ_3 = 4x, 4y; Φ_4 = 2y, 2(−y); receiver = x, −x, −x, x, −x, x, x, −x. Quadrature detection in t_1 and t_2 is obtained with the States method. Gradients were applied as follows: G_1 = 18 G/cm, 500 μs and G_2 = 20 G/cm, 1000 μs. The delay τ is set to 5 ms, and the constant time delay T is set to 25 ms or 40 ms. Solvent suppression was achieved by presaturation.

When combined with NOE data or secondary structure information, useful orientational constraints can be derived.

Methods

Using the 2D CT-COSY experiments described previously (Tian et al., 1999) and assuming the absence of significant differential relaxation, the ^{1}H-^{1}H coupling constants can be obtained from the arctangent of the ratio of cross-peak to auto-peak amplitude divided by πT, where T is the constant time delay ($\arctan(I_{cross}/I_{auto})/\pi T$). Since the cross peaks have antiphase character in a CT-COSY spectrum, a scaling factor is introduced to account for the cancellation effect. This allows the integrated intensity of a spectrum to be used in representing the cross-peak amplitude. Two or more spectra collected with various constant time values allow simultaneous evaluation of the coupling constants and the scaling factors.

The ^{15}N-resolved CT-COSY experiments can be performed by either concatenating a ^{15}N-HSQC before the CT-COSY sequence or in a shared constant time manner (Kay et al., 1992; Kuboniwa et al., 1994), as shown in Figure 1. The sequence of Figure 1 starts by transferring H^{N} magnetization to heteronuclear multiple quantum coherence in a manner analogous to that used in HMQC experiments. Homonuclear ^{1}H-^{1}H couplings dephase coherences to be observed during the whole constant time delay. Both ^{1}H and ^{15}N chemical shift evolutions, reintroduced by moving 180°

pulses, also occur during the constant time period. The shared constant time evolution minimizes sensitivity losses due to relaxation in this 3D experiment. The multiple quantum coherence does not evolve under the influence of the active ^{15}N-^{1}H coupling. Hence, only a single resonance for each site appears in the ^{15}N dimension. The final 90° proton pulse converts antiphase magnetization on the amide proton to antiphase magnetization on coupled remote protons for observation. While water elimination is more problematic in this detection mode, it does provide the highest resolution for measurement of couplings. In addition, since only chemical shifts of amide proton resonances are monitored in the indirect dimension, a smaller spectral width can be used for this dimension.

The evolution of the magnetization in terms of product operators is as follows (only relevant operators are shown):

$$H_z^N \xrightarrow{90_x^H} H_y^N \xrightarrow{\tau} -H_x^N N_z - H_z^i H_y^N N_z$$
$$\xrightarrow{90_x^N} -H_x^N N_y - H_z^i H_y^N N_y \xrightarrow{(T-2\tau),90_x^N}$$
$$H_x^N N_z + H_z^i H_y^N N_z \xrightarrow{\tau} H_y^N - H_y^i H_x^N$$
$$\xrightarrow{90_y^H} H_y^N + H_x^i H_z^N$$

where H^i represents any proton spin coupled to the amide proton. Long-range nitrogen-proton couplings not included in the above description do contribute to evolution during the constant time period but effects are in general small (Sørensen et al., 1997). Also their contributions to the autopeak and cross peak are 90 degrees out of phase with the detected coherence in both indirect dimensions. Such contributions are canceled by the integration procedure described in the Results section.

All NMR spectra were acquired on a Varian Inova spectrometer operating at 800 MHz. A combination of water flipback (Grzesiek and Bax, 1993) and WATERGATE (Piotto et al., 1992) sequences were used for solvent suppression in the NOESY experiment. Water suppression in 2D CT-COSY and 3D ^{15}N-resolved CT-COSY was achieved by presaturation. A 3D HNHA experiment was performed to allow comparison of the couplings measured in the CT-COSY experiment to those measured with a more established method. This experiment was described by Vuister and Bax (1993). Spectra were processed using Felix98 software (MSI).

Data were acquired on both rubredoxin (~5.9 kDa), a Zn-substituted β-sheet iron-sulfur protein from *Pyrococccus furiosus*, and on *E. coli* acyl carrier protein (~8.8 kDa), an α-helical protein involved in fatty acid biosynthesis. ^{15}N labeled and unlabeled recombinant *Pyrococcus furiosus* rubredoxin was produced using the expression vector pTrc99a (Amersham Pharmacia Biotech, Arlington Heights, IL) in *E. coli* NCM533 in minimal media with and without 0.8 g/L $^{15}NH_4Cl$ (>98% ^{15}N, Isotec, Miamisburg, OH) as described previously (Wang et al., 1999). Native *P. furiosus* rubredoxin has the amino terminal methionine cleaved off; however, *E. coli* produces three recombinant forms, wild-type and two unprocessed forms with methionine and formyl-methionine at the amino terminus (Eidsness et al., 1997). Rubredoxin was purified and the three forms separated essentially as described previously (Eidsness et al., 1997), except that a QHP column (Amersham) was used in place of a MonoQ column. Zinc rubredoxin was prepared from the native, iron-containing form as described by Bobak et al. 1989).

^{15}N labeled *E. coli* acyl carrier protein (ACP) was prepared from MgT7-pLysS cells containing the gene for ACP subcloned into a pET11a vector and grown on the minimal medium of Neidhardt et al. (1974). The medium contained 1 g/L of ^{15}N-ammonium chloride (Cambridge Isotope Laboratories) as the sole nitrogen source. The growth and purification of apo-ACP was performed as described by Hill et al. (1995) with a yield of approximately 40 mg of apo-ACP per liter of cell culture. Apo-ACP was checked for purity by SDS-PAGE and lyophilized.

Both bacteriophage and bicelles were used to prepare aligned samples. Phage Pf1 was supplied by Andrej Barbic (Department of Chemistry, Yale University) and grown locally. Pf1 phage was purified following the procedure of Hansen et al. (1998a) and pelleted by ultracentrifugation. The preparation of bicelles is described elsewhere (Losonczi and Prestegard, 1998). Two aligned rubredoxin samples were prepared in this study. The bicelle sample contained 5 mM rubredoxin and 10% DMPC/DHPC (3:1). The phage sample contained 3 mM ^{15}N labeled rubredoxin and enough phage to give a ^{2}H NMR signal with 15 Hz splitting. A 1.8 mM ^{15}N labeled rubredoxin sample was used for the measurement of isotropic $^{3}J(H^{N}H^{\alpha})$ values. The aqueous buffer for these preparations contained 50 mM potassium phosphate at pH 6.3 and 200 mM NaCl. For apo-ACP NMR samples were prepared by exchange into NMR sample buffer using Centricon-3 devices (Amicon) to reach final conditions of 1 mM apo-ACP in 20 mM bis-Tris at pH 6.0, 15 mM $CaCl_2$, 5 mM DTT, 0.02% NaN_3, and 10%

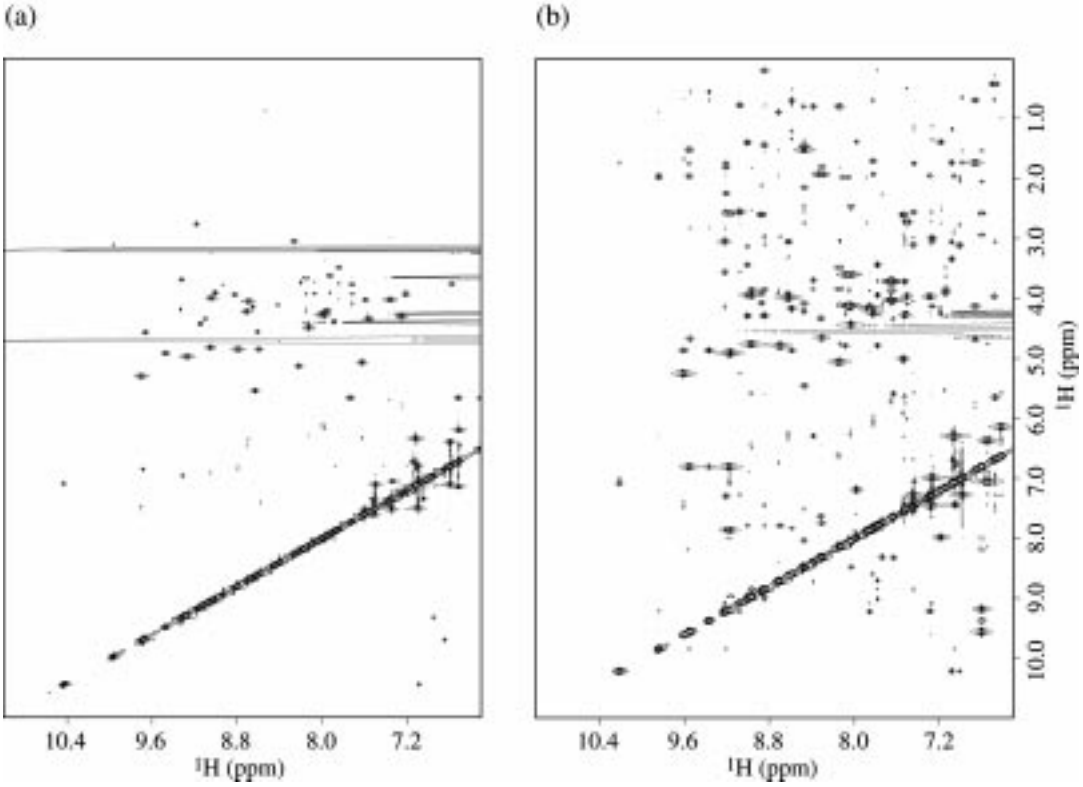

Figure 2. Contour plots of the 2D CT-COSY spectra of rubredoxin in dilute bicelle media (a) at 25 °C showing the isotropic J coupling connectivities and (b) at 42 °C showing dipolar coupling connectivities. The spectra were acquired on a 5 mM sample with 10650 Hz spectral width in both dimensions, 24 scans per FID, 1.2 s recycle delay, 2048× 256 complex points, which were zero filled to 4096 × 512.

D_2O (Isotec). Enough Pf1 phage was added to the sample to give a ^{2}H NMR signal with 15 Hz splitting.

Results

^1H-^1H dipolar couplings in proteins

Many proton spins in proteins are close in space. Sequential H^{α}-H^N distances in β-sheets and sequential H^N-H^N distances in α-helices and turns are less than 3 Å. Anisotropic tumbling of proteins in weakly field-oriented media will result in significant residual ^{1}H-^{1}H dipolar couplings in these cases, and cross peaks from through-space interactions should be observable in COSY spectra. As an example, a 2D CT-COSY spectrum of rubredoxin in 10% DMPC/DHPC bicelle solution at 42 °C is shown in Figure 2b. The auto-peaks are shown absorptive, in-phase, in both dimensions; consequently, the cross peaks are absorptive, in-phase, in the indirect dimension and dispersive, antiphase, in the direct dimension. Although no attempt is made to fully assign the cross peaks, they clearly include both inter- and intraresidue H^{α}-H^N, H^{β}-H^N and sequential H^N-H^N connectivities. In comparison, a 2D CT-COSY spectrum recorded on the same sample in isotropic phase (at 25 °C) is shown in Figure 2a. Only through-bond connectivities such as intraresidue H^{α}-H^N connectivities are observed. The additional cross peaks in Figure 2b come from coherence transfer mediated by residual ^{1}H-^{1}H dipolar couplings. These through-space couplings are averaged to zero for randomly tumbling molecules and therefore they are not observable in isotropic solution.

Comparison of CT-COSY and NOESY experiments

Traditionally, NOE based experiments have been the only means for obtaining through-space connectivities by NMR. Such information is now also available from CT-COSY experiments in weakly aligned media. Both 2D NOESY and CT-COSY spectra were recorded on ACP aligned in a solution of Pf1 phage. Because ACP is predominantly α-helical (Holak et al., 1988; Kim and Prestegard, 1990), extensive H^N-H^N cross peaks should be observed in the NOESY spec-

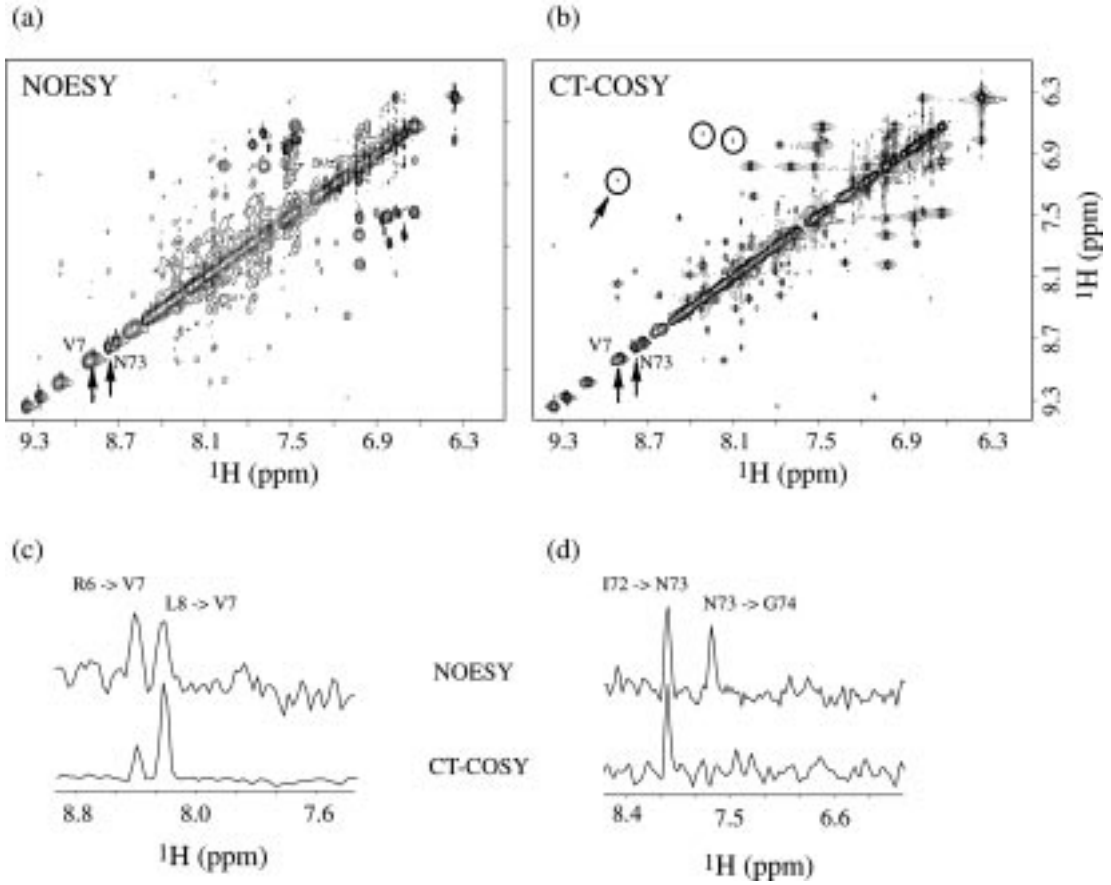

Figure 3. Sections of the (a) NOESY and (b) 2D CT-COSY spectra of ^{15}N labeled acyl carrier protein in phage solution. Slices along the indirect proton dimension from both spectra were taken at residues (c) Val7 and (d) Asn73. Peaks present only in the CT-COSY are circled. The spectra were acquired on a 1.5 mM sample with 9000 Hz spectral width in both dimensions, 160 scans per FID, 1.2 s recycle delay, 2048 × 240 complex points, which were zero filled to 4096 × 512. A 100 ms mixing time was used in the NOESY experiment, and a 25 ms constant time delay was used in the CT-COSY experiment.

trum. The amide regions of both spectra are shown in Figure 3. The two spectra were acquired on the same sample with approximately equal amounts of spectrometer time. About the same number of H^N-H^N cross peaks are observed in the CT-COSY spectrum (Figure 3b), which suggests these two experiments have comparable sensitivity overall. Slices along the ω1 dimension through the peak corresponding to Val7 from both NOESY and CT-COSY spectra (Figure 3c) suggest the sensitivity of the CT-COSY experiment to be somewhat better. Val7 is part of the first helix in ACP. Sequential H^N-H^N connectivities from residues 6 to 7 and residues 7 to 8 are observed.

Slices along the ω1 dimension through residue Asn73 are shown in Figure 3d. Asn73 is part of helix III in ACP. The sequential H^N-H^N cross peaks of Ile72 to Asn73 and Asn73 to Gly74 are observed in the NOESY spectrum. But only the H^N-H^N cross-peak of Ile72 to Asn73 is seen in the CT-COSY spectrum. While this suggests lower sensitivity for the CT-COSY experiment in this case, it also represents an example of the complementary information provided by NOESY and CT-COSY experiments. While cross-peak amplitudes in NOESY only depend on the ^{1}H-^{1}H distance, in CT-COSY they depend on both the distance and the orientation of the internuclear vector with respect to the magnetic field. If the internuclear vector points in particular directions relative to the alignment frame (at the magic angle for an axially symmetric system), the dipolar coupling will be zero regardless of proximity of spin pairs. In this case, while the NOESY experiment indicates H^N-H^N distances from Ile72 to Asn73 and from Asn73 to Gly74 to be similar, the CT-COSY experiment suggests that

these two internuclear vectors have different average orientations with respect to the magnetic field.

A few circled cross peaks are present in the CT-COSY spectrum that are not in the NOESY spectrum. The circled cross peak indicated by an arrow is from an interaction between H^{ζ} Phe50 and the Val7 H^N, 4 to 5 Å away. Because of the $1/r^3$ distance dependence of directly observed dipolar couplings in the CT-COSY experiment, as opposed to the $1/r^6$ dependence of NOEs, longer distances can be observed in CT-COSY if the internuclear vectors are optimally aligned (vector parallel to the field). Long-distance ^{1}H-^{1}H dipolar interactions have been previously observed in nucleic acids as well (Hansen et al., 1998b).

3D ^{15}N resolved CT-COSY experiment

For larger proteins resolution will become an issue and 3D ^{15}N resolved CT-COSY experiments will become important. An ω2, ω3 plane from the 3D ^{15}N resolved CT-COSY spectrum of rubredoxin in phage solution at a ^{15}N shift of 122.6 ppm is shown in Figure 4A. In addition to the intraresidue H^N-H^α connectivities, a sequential cross peak from W3H^α to V4H^N is observed. This is what we expect for residues Trp3 and Val4, which are involved in a β-sheet secondary structure. In Figure 4B, an ω2, ω3 plane from the 3D ^{15}N resolved CT-COSY spectrum of ACP in phage solution at a ^{15}N shift of 118.2 ppm is shown. As we expected for an α-helical protein, a significant number of cross peaks, including intraresidue H^α-H^N, sequential H^α–H^N and sequential H^N-H^N cross peaks, are observed.

Quantitative measurement of couplings

In some cases, it will be useful to make a quantitative evaluation of the observed couplings. This could be a challenging problem. As shown in Figure 2 and 3, the proton-proton couplings in aligned media can be quite extensive. For example, it is very common that an amide proton in aligned media will couple to both intra- and inter- residue alpha protons, side-chain protons and other amide protons, instead of just its own H^α. The magnitude of coupling also has a wide range. The sequential H^α-H^N dipolar couplings in β-sheets, sequential H^N-H^N dipolar couplings in α-helices, H^α-H^β couplings and side-chain ^{1}H-^{1}H couplings can be on the same order as one-bond ^{15}N-^{1}H dipolar couplings. Because of the extensive sets of couplings, measurement of the ^{1}H-^{1}H couplings has to take passive coupling effects into account. The CT-COSY experiment described in our previous study is one way of doing this. Appropriate procedures for analyzing

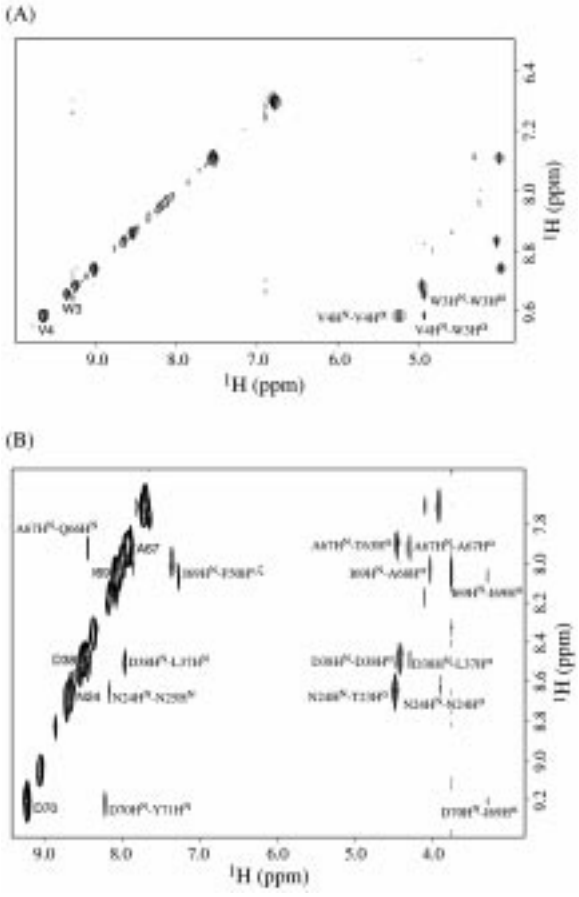

Figure 4. (A) An ω2, ω3 plane from the 3D ^{15}N resolved CT-COSY spectrum of ^{15}N labeled rubredoxin in phage solution at $^{15}N = 122.6$ ppm. The spectrum was acquired on a 3 mM sample with spectral widths of 10650 Hz in ω3, 6000 Hz in ω2 and 3200 Hz in ω1, 8 scans per FID, 1.2 s recycle delay, 25 ms constant time delay, 1024 × 64 × 16 complex points. ω2 and ω1 were linear predicted to 128 and 32 points, respectively, and then the data were zero filled for a final matrix size of 2048 × 256 × 64. The proton carrier frequency was at 8.0 ppm in t_1 and t_2, and moved to 4.7 ppm (water resonance) in t_3. (B) An ω2, ω3 plane from the 3D ^{15}N resovled CT-COSY spectrum of ^{15}N labeled apo-ACP in phage solution at $^{15}N = 118.2$ ppm. The spectrum was acquired on a 1.5 mM sample with spectral width of 10650 Hz in ω3, 5600 Hz in ω2 and 3200 Hz in ω1, 24 scans per FID, 1.2 s recycle delay, 25 ms constant time delay, 1024 × 48 × 18 complex points. ω2 and ω1 were linear predicted to 64 and 32 points, respectively, and then the data were zero filled for a final matrix size of 1024 × 128 × 64. The proton carrier frequency was at 6.7 ppm in t_1 and t_2, and moved to 4.7 ppm (water resonance) in t_3.

the ratio of cross and auto peaks allow one to eliminate most effects of passive couplings. These procedures require introduction of a scaling factor to account for cancellation of antiphase components in the cross peaks.

In our previous study a set of spectra with various constant time delays were collected to evaluate the coupling constant and the scaling factor, but in the study of proteins it is more practical to acquire two spectra. Spectra with 25 ms and 40 ms constant time delays were recorded to measure $^3J(H^NH^\alpha)$ couplings in rubredoxin. Only those peaks which are well resolved, are not close to the water resonance, and have a signal-to-noise ratio higher than 20 in both spectra were used in the quantitative analysis. The autopeaks were phased absorptive and directly integrated to represent the autopeak amplitude. For cross peaks, the positive and negative components of the multiplets are integrated separately and the sum of the absolute intensities of these components is used to represent the cross-peak amplitude. The ratios of the amplitudes at two delays were then used to directly solve $I_{cross}/I_{auto} = A\tan[\pi(J+D)T]$ for the coupling (J + D) and the scaling factor A.

A list of representative $^3J(H^NH^\alpha)$ values for rubredoxin measured by 3D ^{15}N resolved CT-COSY in isotropic solution is presented in Table 1. For comparison purposes, $^3J(H^NH^\alpha)$ values measured by HNHA experiments and the calculated values from an X-ray structure (1BRF, Bau et al., 1998) are also listed. The rmsd between the values measured by the ^{15}N CT-COSY and the HNHA experiments is 0.6 Hz, with the largest deviation being 1.3 Hz. Both measurement approaches give values showing moderate and equally good agreement with couplings calculated from the Karplus equation using dihedral angles taken from the crystal structure of the native Fe-protein. In our hands, for residues with $^3J(H^NH^\alpha)$ larger than 4 Hz, the cross peaks have sufficient signal to noise for reliable measurements. For those residues where quantitative measurements are not possible, qualitative estimates can be made.

As an additional demonstration of the validity of the coupling measurements, we compare measured values of the backbone ^{1}H-^{1}H dipolar couplings from spectra on rubredoxin aligned in phage to values calculated using an X-ray structure. For cross peaks present in both aligned and isotropic spectra, both the sign and magnitude of dipolar couplings can be determined based on the known sign of the J-couplings. For example, the H^N-H^α coupling of residue Val4 from data in Figure 4 is measured to be $+/-$ 11.4 Hz in the aligned phase. The $^3J(H^NH^\alpha)$ coupling measured in the isotropic phase is 9.4 Hz. Thus, the residual H^N-H^α dipolar coupling could be 2.0 or -20.8 Hz. The degree of order in this sample is not high enough to produce couplings as large as -20.8 Hz, so the dipolar contribution must be 2.0 Hz. For those cross peaks only present in aligned spectra, we can determine their magnitudes, although advances in methods for determining signs of couplings have been made recently (Otting et al., 2000). The calculated couplings were obtained using the X-ray structure (1BRF, Bau et al., 1998) and an alignment tensor from analysis of the one-bond ^{15}N-^{1}H couplings using the program *dynamics* (available at our web site: www.tesla.uga.edu). The axial and rhombic components of the alignment were -0.00038 and -0.00019, respectively. For those cou-

Table 1. Comparison of measured $^3J(H^NH^\alpha)$ coupling constants for some residues of rubredoxin from 3D ^{15}N resolved CT-COSY and HNHA experiments

Residue	^{15}N-CT-COSY	HNHA	Karplus
Trp3	9.2	9.5	9.7
Val4	9.4	9.6	9.2
Cys5	3.8	3.3	6.0
Cys8	10.5	9.5	9.9
Ala16	7.1	8.4	8.2
Asn21	9.6	10.0	9.6
Glu31	9.2	8.7	7.6
Trp36	3.6	4.2	4.8
Val37	9.4	9.2	9.6
Ile40	8.4	8.3	7.8
Lys-45	4.8	4.2	3.5
Phe48	8.9	8.8	9.2

The 3D HNHA (Vuister and Bax, 1993) spectrum was acquired with spectral widths of 9600 Hz in ω3, ω2 and 2800 Hz in ω1. Two 3D ^{15}N-resolved CT-COSY spectra with 25 ms and 40 ms constant time delays were recorded with spectral widths of 9600 Hz in ω3, 5600 Hz in ω2 and 2800 Hz in ω1. The proton carrier frequency was placed at 8.0 ppm in t_1 and t_2, and moved to 4.7 ppm (water resonance) in t_3. Other experimental parameters are 8 scans per FID, 1.2 s recycle delay, 1024 × 36 × 16 complex points. ω2 and ω1 were linear predicted to 64 and 32 points, respectively, and then the data were zero filled for a final matrix size of 1024 × 128 × 64. The presented values are not corrected for differential relaxation effects which result in slightly reduced values for the HNHA experiment. These experiments were performed on a 1.8 mM rubredoxin sample. J-coupling values from the X-ray structure (1BRF) were calculated using the Karplus relationship (Vuister and Bax, 1993).

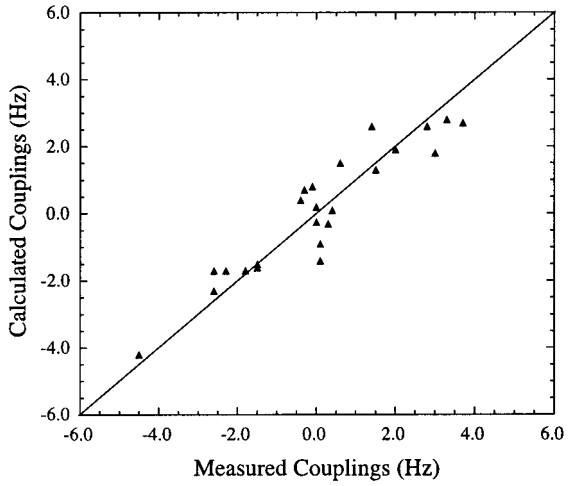

Figure 5. Plot of the measured dipolar couplings for rubredoxin in phage solution versus the predicted values from the X-ray structure. The correlation coefficient is 0.93.

plings which have undetermined signs, we assume that the measured values have the same signs as the predicted couplings. Results presented in Figure 5 show excellent agreement.

Discussion

The data presented above illustrate that CT-COSY-based experiments on weakly aligned proteins can be used to directly observe the proton-proton connectivities mediated by residual dipolar couplings with an overall sensitivity comparable to NOESY experiments. The same experiment can give a quantitative measure of homonuclear residual dipolar couplings including intra- and interresidue $^{1}H^{N}$-$^{1}H^{\alpha}$ couplings and sequential $^{1}H^{N}$-$^{1}H^{N}$ couplings.

There are some alternative approaches to quantitative coupling measurement, including ones that extract coupling constants from frequency domain spectra (Kim and Prestegard, 1989; Eberstadt et al., 1995; Andrec and Prestegard, 1998) and E. COSY-like experiments (Willker and Leibfritz, 1992; Weisemann et al., 1994; Griesinger et al., 1985). Although the latter experiments have some nice features, such as determining the sign of the couplings, they either require additional ^{13}C-labeling (Cai et al., 1999) or rely on TOCSY or NOE mixing for generating cross peaks (Meissner et al., 1997; Sørensen et al., 1997; Peti and Griesinger, 2000). To our knowledge, they have not been used to measure H^{N}-H^{N} couplings. In α-helices and turns, the H^{N}-H^{N} couplings are expected to be significant.

The HNHA experiment is also used routinely for the measurement of $^{3}J(H^{N}H^{\alpha})$ couplings. Some proton-proton dipolar couplings measured from the HNHA experiment have been used recently for structure refinement (Tjandra et al., 2000). However, there is a concern that application may be complicated for multiply dipolar coupled spin systems since passive couplings evolving during the proton indirect dimension evolution period are typically neglected (Vuister and Bax, 1993). Neglect is based on an ability to use a short evolution time during which small passive couplings have little effect. However, in aligned media the numbers of couplings can be substantial and some of the couplings can be quite large. Short evolution times also result in poor digital resolution in the indirect proton dimension. While poor resolution is not a problem for measuring couplings from the single H^{N}-H^{α} cross peaks that occur in isotropic solution, it will cause overlap of the multiple cross peaks seen along the indirect proton dimension in weakly aligned media.

When both data sets are available, the CT-COSY experiments shown here nicely complement NOESY experiments. First, the connectivities in CT-COSY experiments can identify NOE cross-peaks that may arise from spin-diffusion. Second, due to the $1/r^{3}$ dependence of the dipolar interaction, the connectivities in CT-COSY experiments may extend to longer distances. The additional peaks in CT-COSY can provide very useful long-range structural information. Third, for spin pairs with a well defined distance, the dipolar couplings measured from CT-COSY experiments give orientational information for internuclear vectors. We expect this latter type of information to be abundant and very useful. A recent statistical analysis of NMR data indicates that short- and medium-range NOEs have a completeness of 90% and 75%, respectively (Doreleijers et al., 1999). Since sequential $^{1}H\alpha$-$^{1}H^{N}$ distances in β-sheets and $^{1}H^{N}$-$^{1}H^{N}$ distances in α-helices are short-range, the number of dipolar connections should be quite large. We have been able to obtain a significant number of proton-proton dipolar couplings from ACP labeled only with ^{15}N. In combination with the one-bond ^{15}N-^{1}H couplings, the backbone folding is quickly determined (data to be published) using a combination of the orientational constraints derived from the residual dipolar couplings and a few distance constraints derived from NOE data.

Demonstrations presented here have been restricted to small proteins. For larger systems, the short transverse relaxation time will decrease the sensitivity of the CT-COSY experiment. However, at least for deuterated proteins a higher level of alignment can be used without significant line broadening (Wang et al., 1998). Thus, observation of H^N-H^N connectivities in CT-COSY experiments should still be feasible. In addition, some loss in sensitivity might be regained by adoption of TROSY-based methods (Pervushin et al., 1997). Redesign of 3D ^{15}N-resolved CT-COSY experiments, which currently are based on HMQC-style experiments, is currently being explored.

Acknowledgements

This work was supported by grants from the National Science Foundation MCB-9726341 and MCB-9809060, and benefited from instruments made available through the Georgia Research Alliance. We would like to thank the University of Georgia metalloenzyme group for useful discussions on the properties of rubredoxin.

References

Andrec, M. and Prestegard, J.H. (1998) *J. Magn. Reson.*, **130**, 217–232.

Bau, R., Rees, D.C., Kurtz, D.M., Scott, R.A., Huang, H., Adams, M.W.W. and Eidsness, M.K. (1998) *J. Biol. Inorg. Chem.*, **3**, 484–493.

Bobak, D.A., Nightingale, M.S., Murtagh, J.J., Price, S.R., Moss, J., and Vaughan, M. (1989) *Proc. Natl. Acad. Sci. USA*, **86**, 6101–6105.

Cai, M., Wang, H., Olejniczak, E.T., Meadows, R.P., Gunasekera, A.H., Xu, N. and Fesik, S.W. (1999) *J. Magn. Reson.*, **139**, 451–453.

Clore, G.M., Gronenborn, A.M. and Tjandra, N. (1998) *J. Magn. Reson.*, **131**, 159–162.

Doreleijers, J.F., Raves, M.L., Rullmann, T. and Kaptein, R. (1999) *J. Biomol. NMR*, **14**, 123–132.

Eberstadt, M., Gemmecker, G., Mierke, D. and Kessler, H. (1995) *Angew. Chem. Int. Ed. Engl.*, **34**, 1671–1695.

Eidsness, M.K., Richie, K.A., Burden, A.E., Kurtz, D.M. and Scott, R.A. (1997) *Biochemistry*, **36**, 10406.

Griesinger, C., Sørensen, O.W. and Ernst, R.R. (1985) *J. Am. Chem. Soc.*, **107**, 6394–6396.

Grzesiek, S. and Bax, A. (1993) *J. Am. Chem. Soc.*, **115**, 12593–12594.

Hansen, M.R., Mueller, L. and Pardi, A. (1998a) *Nat. Struct. Biol.*, **5**, 1065–1074.

Hansen, M.R., Rance, M. and Pardi, A. (1998b) *J. Am. Chem. Soc.*, **120**, 11210–11211.

Hill, R.B., MacKenzie, K.R., Flanagan, J.M., Cronan, J.E., Jr. and Prestegard, J.H. (1995) *Protein Expr. Purif.*, **6**, 394–400.

Holak, T.A., Kearsley, S.K., Kim, Y. and Prestegard, J.H. (1988) *Biochemistry*, **27**, 6135–6142.

Kay, L.E., Wittekind, M., McCoy, M.A., Friedrichs, M.S. and Mueller, L. (1992) *J. Magn. Reson.*, **98**, 443–450.

Kim, Y. and Prestegard, J.H. (1989) *J. Magn. Reson.*, **84**, 9–13.

Kim, Y. and Prestegard, J.H. (1990) *Proteins*, **8**, 377–385.

Kuboniwa, H., Grzesiek, S., Delaglio, F. and Bax, A. (1994) *J. Biomol. NMR*, **4**, 871–878.

Losonczi, J.A. and Prestegard, J.H. (1998) *J. Biomol. NMR*, **12**, 447–451.

Meissner, A., Duus, J. and Sørensen, O.W. (1997) *J. Magn. Reson.*, **128**, 92–97.

Neidhardt, F.C., Bloch, P.L. and Smith, D.F. (1974) *J. Bacteriol.*, **119**, 736–747.

Ottiger, M., Delaglio, F. and Bax, A. (1998) *J. Magn. Reson.*, **131**, 373–378.

Otting, G., Rückert, M., Levitt, M. and Moshref, A. (2000) *J. Biomol. NMR*, **16**, 343–346.

Pellecchia, M., Kooi, C.W.V., Keliikuli, K. and Zuiderweg, E.R.P. (2000) *J. Magn. Reson.*, **143**, 435–439.

Pervushin, K., Riek, R., Wider, G. and Wüthrich, K. (1997) *Proc. Natl. Acad. Sci. USA*, **94**, 12366–12371.

Peti, W. and Griesinger, C. (2000) *J. Am. Chem. Soc.*, **122**, 3975–3976.

Piotto, M., Saudek, V. and Sklenár, V. (1992) *J. Biomol. NMR*, **2**, 661–665.

Prestegard, J.H. (1998) *Nat. Struct. Biol.*, **5**, 517–522.

Sali, A. and Kuriyan, J. (1999) *Trends Biochem. Sci.*, **24**, M20–M24.

Sørensen, M., Meissner, A. and Sørensen, O.W. (1997) *J. Biomol. NMR*, **10**, 181–186.

Tian, F., Bolon, P. and Prestegard, J. (1999) *J. Am. Chem. Soc.*, **121**, 7712–7713.

Tjandra, N. and Bax, A. (1997) *Science*, **278**, 1111–1114.

Tjandra, N. and Bax, A. (1997) *J. Magn. Reson.*, **124**, 512–515.

Tjandra, N., Marquardt, J. and Clore, G.M. (2000) *J. Magn. Reson.*, **142**, 393–396.

Tolman, J.R., Flanagan, J.M., Kennedy, M.A. and Prestegard, J.H. (1995) *Proc. Natl. Acad. Sci. USA*, **92**, 9297–9283.

Tolman, J.R. and Prestegard, J.H. (1996) *J. Magn. Reson.*, **B112**, 245–252.

Vuister, G.W. and Bax, A. (1993) *J. Am. Chem. Soc.*, **115**, 7772–7777.

Wang, P.L., Calzolai, L., Bren, K.L., Teng, Q., Jenney, J.F.E., Brereton, P.S., Howard, J.B., Adams, M.W.W. and Lamar, G.N. (1999) *Biochemistry*, **38**, 8167–8178.

Wang, Y.X., Marquardt, J.L., Wingfield, P., Stahl, S.J., Huang, S., Torchia, D. and Bax, A. (1998) *J. Am. Chem. Soc.*, **120**, 7385–7386.

Weisemann, R., Ruterjans, H., Schwalbe, H., Schleucher, J., Bermel, W. and Griesinger, C. (1994) *J. Biomol. NMR*, **4**, 231–240.

Willker, W. and Leibfritz, D. (1992) *J. Magn. Reson.*, **99**, 421–425.

Wüthrich, K. (1986) *NMR of Proteins and Nucleic Acids*, Wiley, New York, NY.